Electronic Supplementary Material (ESI) for Physical Chemistry Chemical Physics.

Using Ion-Selective Membranes to Study Cation Transport in Hybrid Organic-Inorganic Perovskites

*Emily C. Smith, Christie L.C Ellis, Hamza Javaid, Blaise G. Arden, D. Venkataraman**

Department of Chemistry, University of Massachusetts Amherst, Amherst Massachusetts 01003-9303, United States

AUTHOR INFORMATION

Corresponding Author

*(D. Venkataraman). E-mail: dv@umass.edu

Using Ion-Selective Membranes to Study Cation Transport in Hybrid Organic-Inorganic Perovskites

Supplementary Information

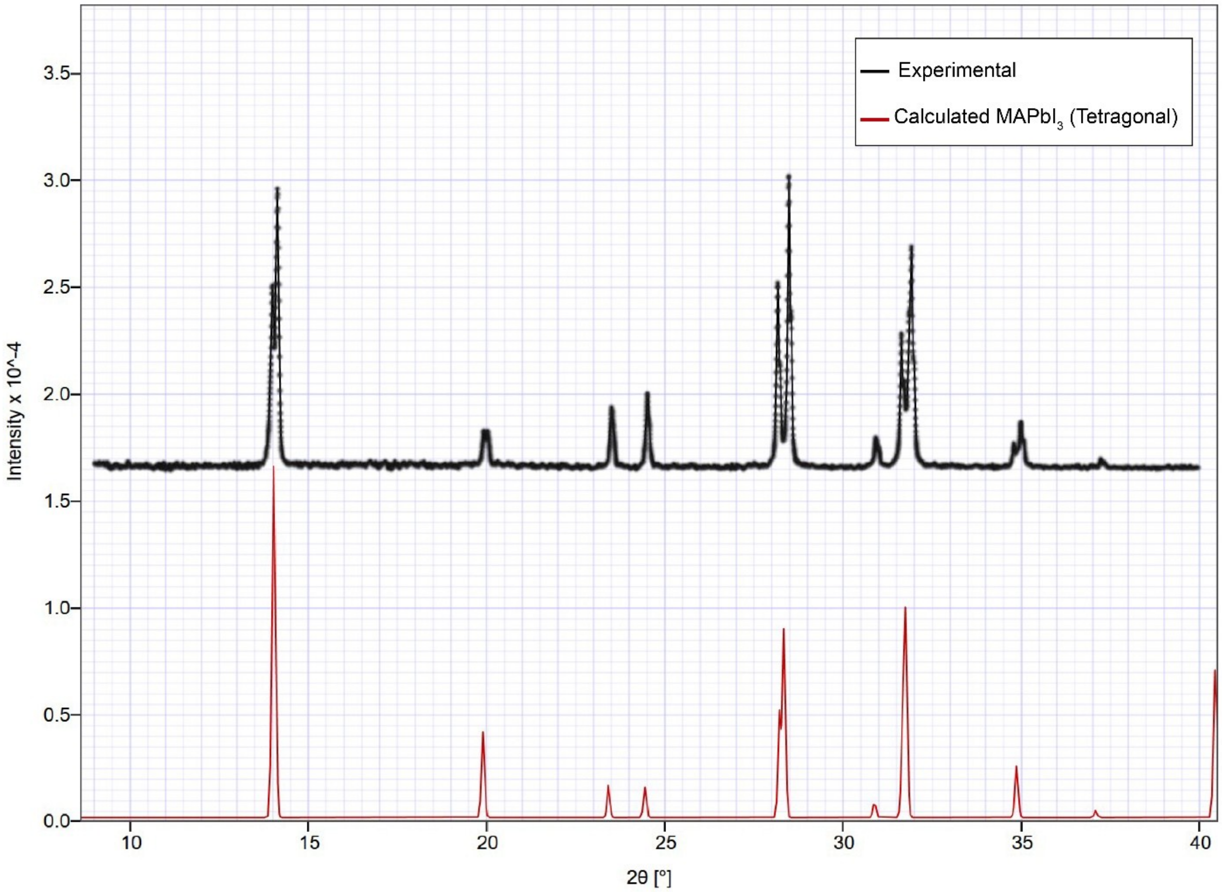

Figure S1. Experimental powder x-ray diffraction of MAPbI$_3$ powder (black) and calculated diffraction for MAPbI$_3$ in the tetragonal phase (red).

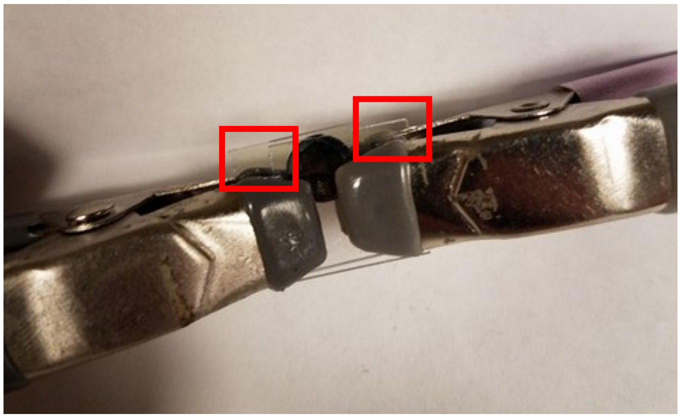

Figure S2. Picture of a real device with ISM coated ITO glass slides sandwiching a $MAPbI_3$ pellet. Leads are clipped to both ITO substrates from the exposed ends (shown by the red boxes). The ISM coating these portions is scraped away before attaching leads.

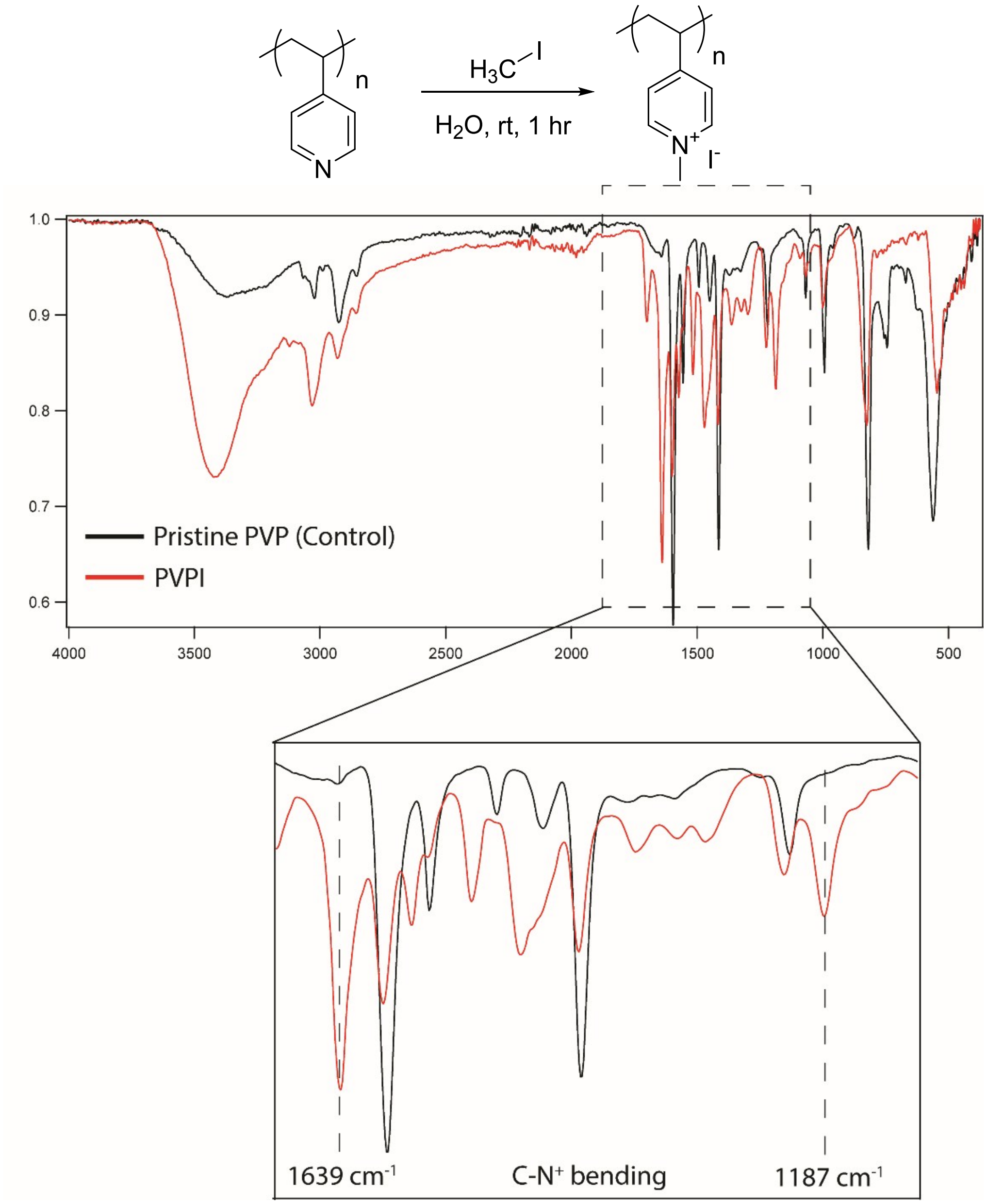

Figure S3. FTIR spectra of poly(4-vinylpyridine) before (black) and after (red) methylation to form the quaternary amine product (PVPI). Unique peaks at 1639 cm^{-1} and 1187 cm^{-1} appear in this sample and are attributed to the C-N$^+$ bending response.

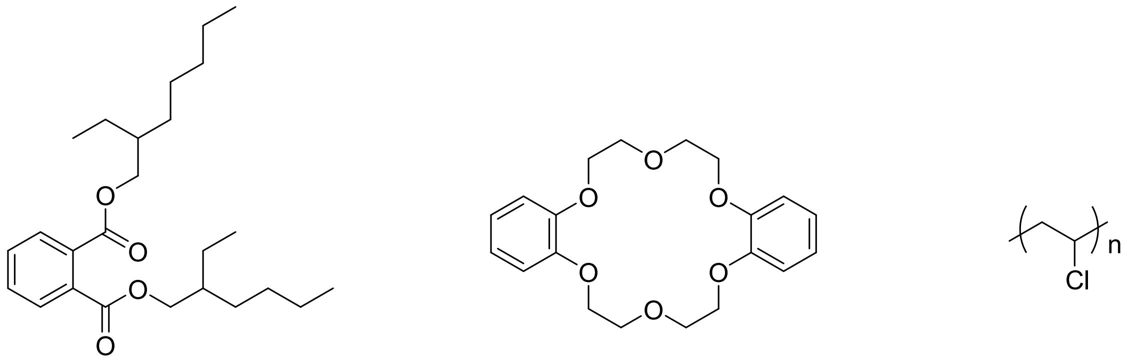

bis(2-ethylhexyl)phthalate (DEHP) dibenzo-18-crown-6 (DB18C6) polyvinyl chloride

Figure S4. Chemical structure of ISM components: polyvinyl chloride (PVC) as an electronically insulating scaffold material, bis(2-ethylhexyl)phthalate (DEHP) as a membrane solvent, and dibenzo-18-crown-6 (DB18C6) as a cation-selective ionophore.

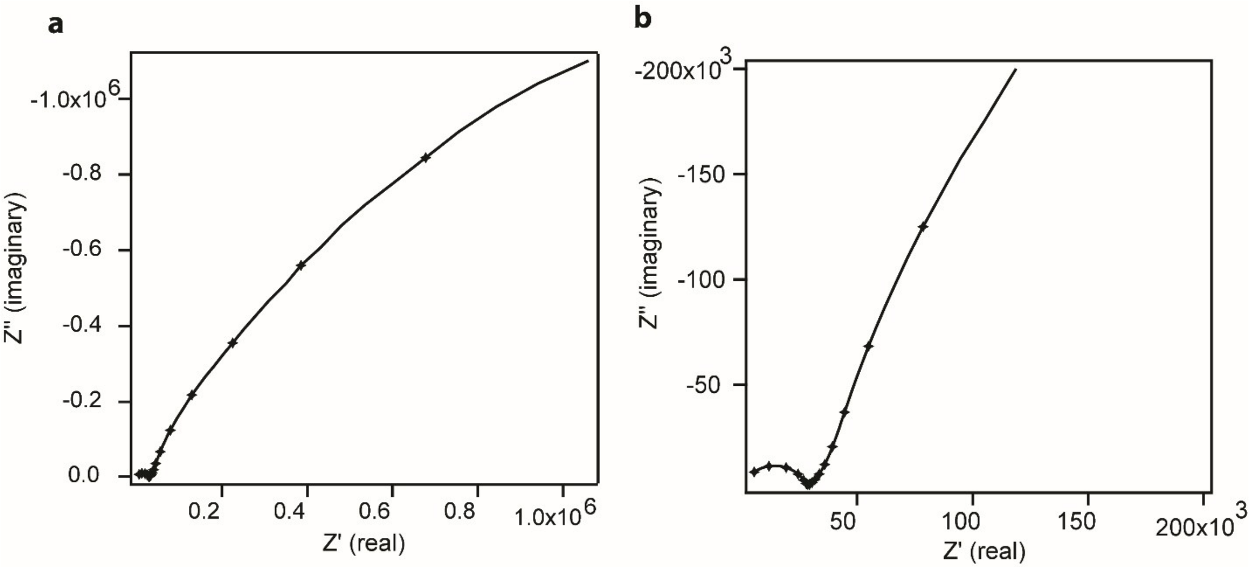

Figure S5. (a) EIS response as a Nyquist plot of a pristine $MaPbI_3$ pellet sandwiched between two clean ITO substrates (b) The EIS response of the same sample zoomed into the high frequency region.

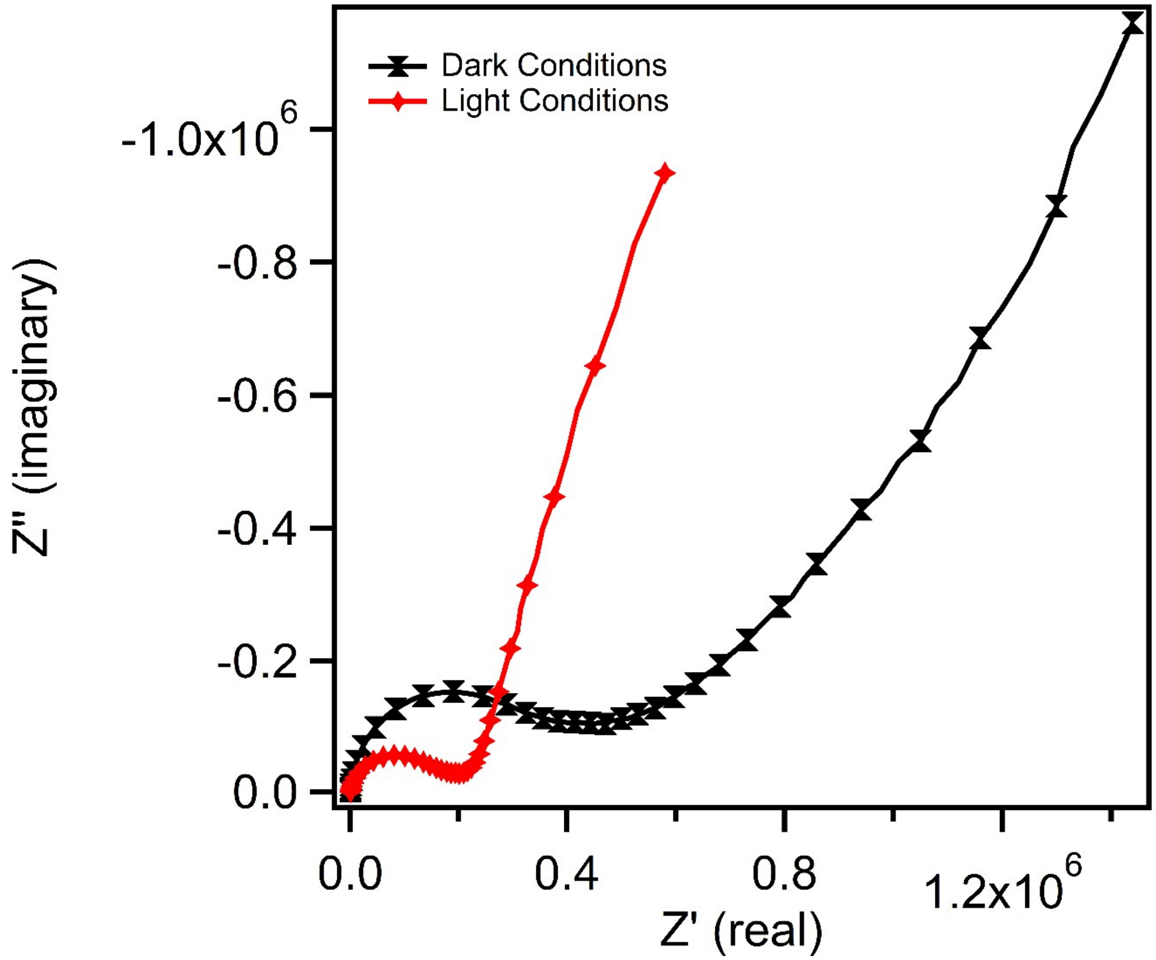

Figure S6. The EIS response as a Nyquist plot of a $MAPbI_3$ pellet sandwiched between two ISM coated electrodes in the dark (black hourglass) and under illumination with a 100 W incandescent lightbulb (red stars).

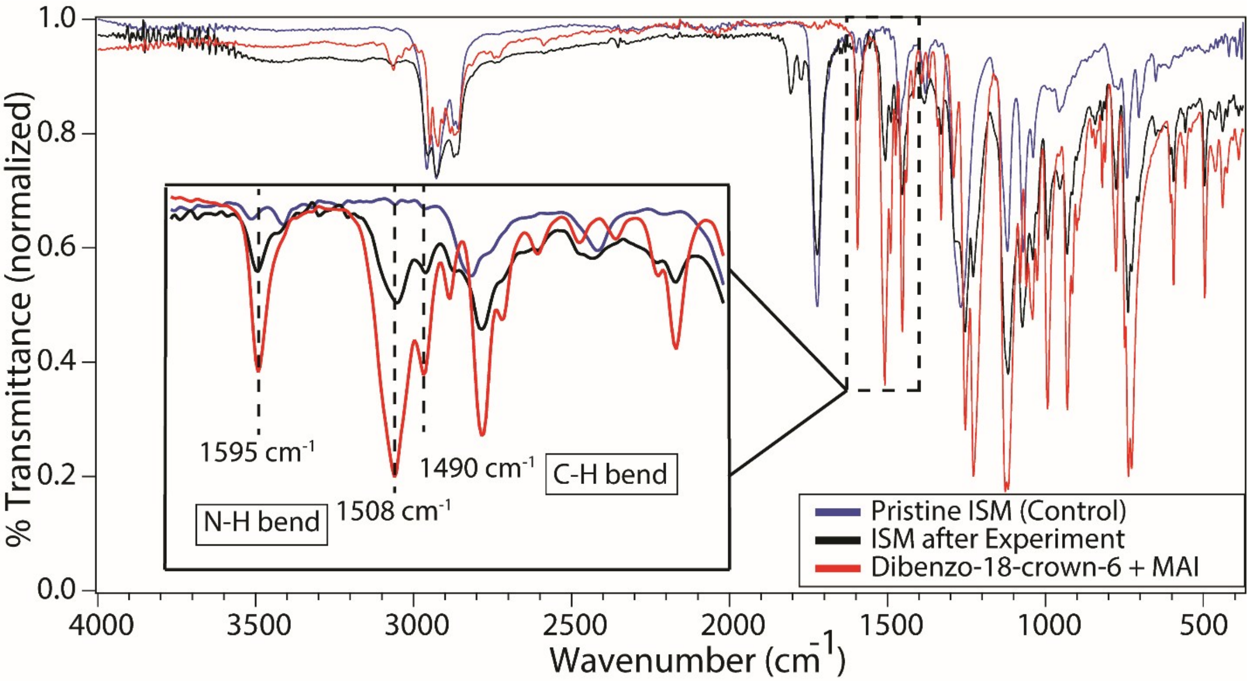

Figure S7. FTIR of the ISM before (blue) and after (black) being exposed to $MAPbI_3$ under illumination at 1.5 V bias for 12 h. A positive control of DB18C6 and MAI is shown in red.

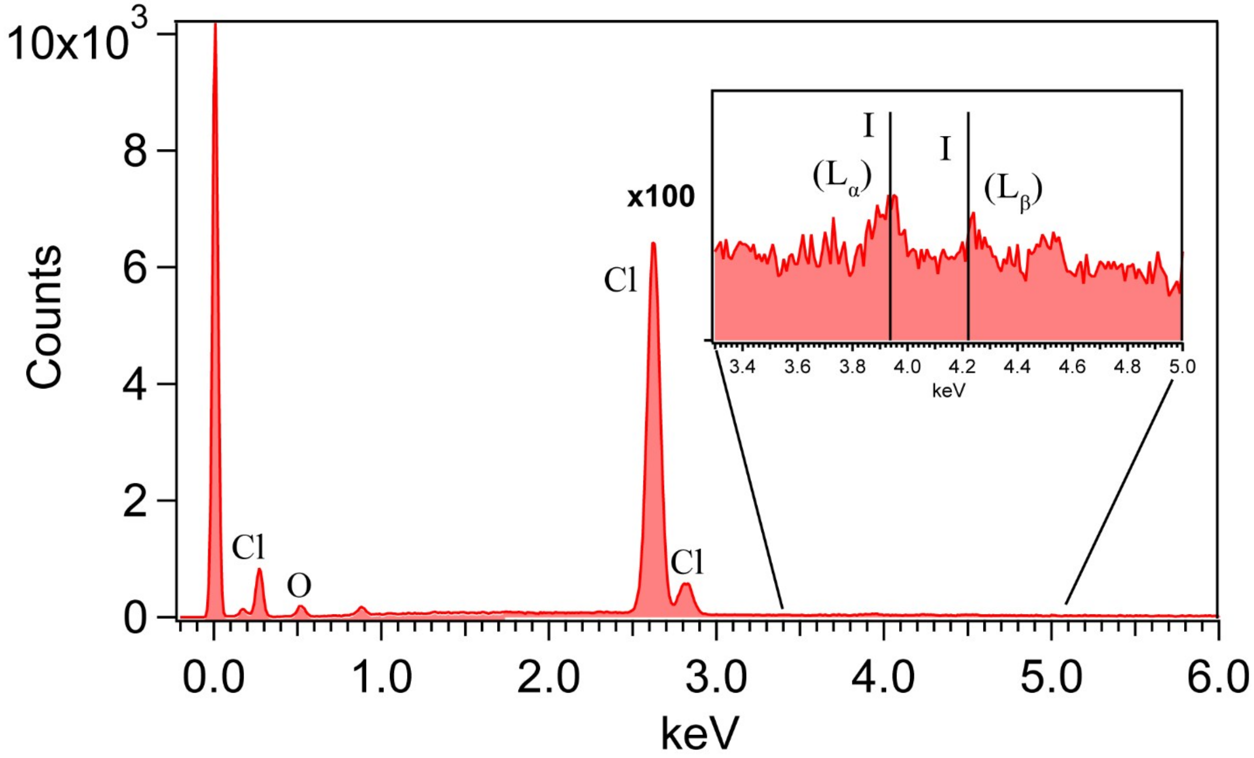

Figure S8. EDX analysis of a membrane after being exposed to the HOIP sample under constant illumination at 1.5 V for 24 h. Known iodine peaks corresponding to L_α (3.938 keV) and L_β (4.221 keV) emissions are denoted in black.

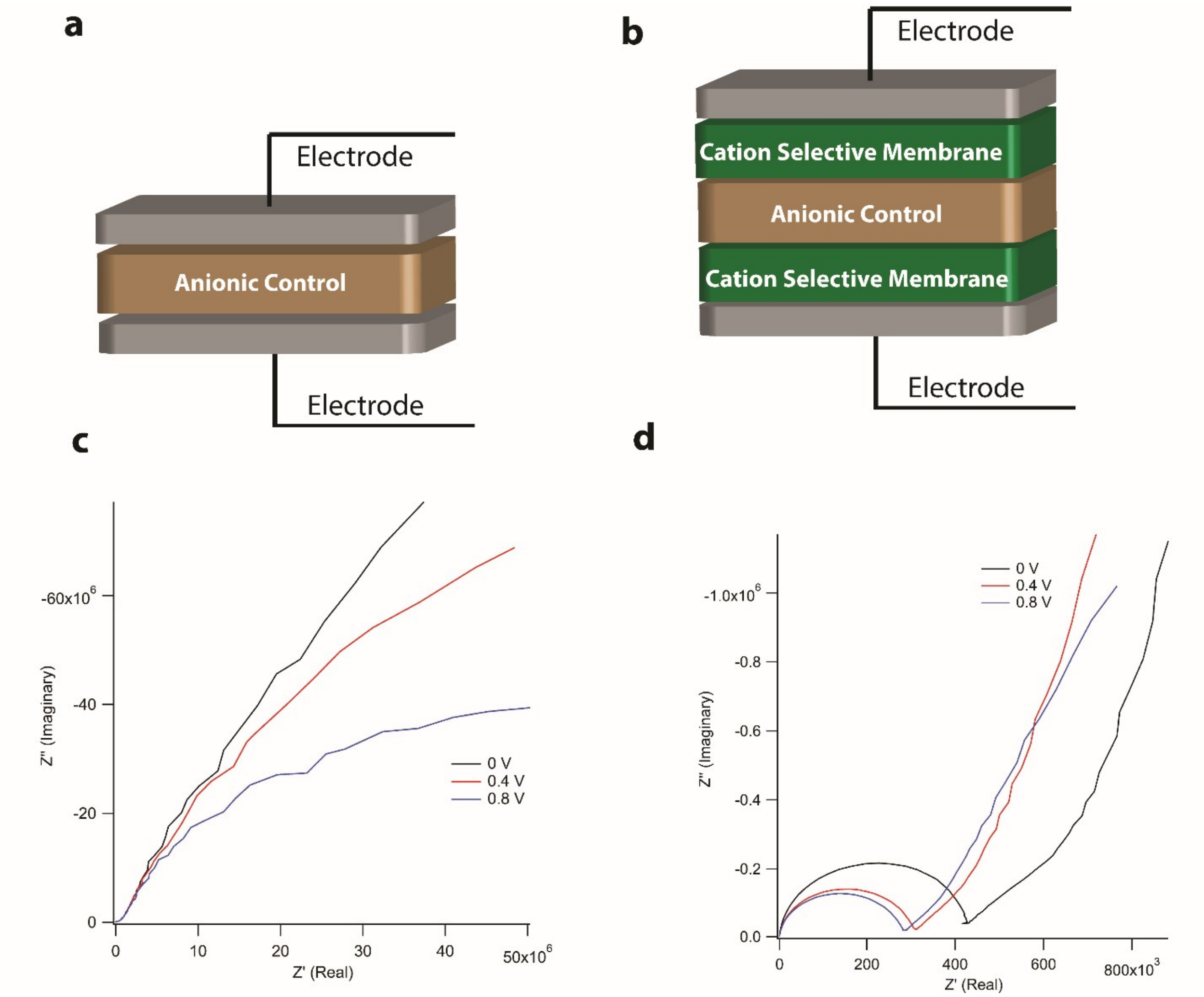

Figure S9. Schematics of the anion controls with (a) and without (b) the ISM. (c) The impedance response of the anionic control without the ISM at varying applied bias 0 (black), 0.4 V (red), and 0.8 V (blue). (d) The impedance response of the anionic control with the ISM at varying applied bias 0 (black), 0.4 V (red), and 0.8 V (blue). The structure of the control can be found in Figure S3.

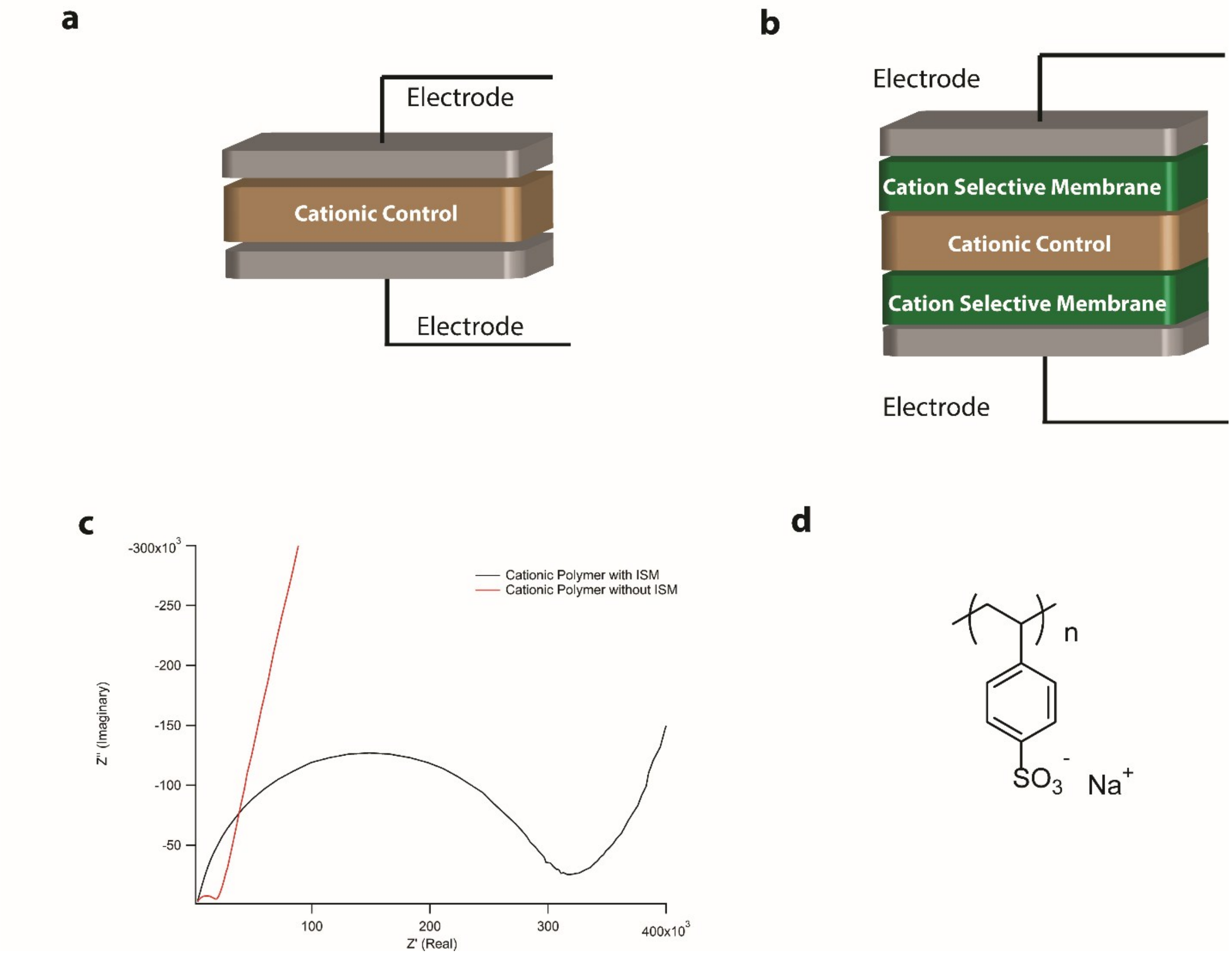

Figure S10. Schematics of the anion controls with (a) and without (b) the ISM. (c) The impedance response of the cationic control without (small, red) and with (large, black) the ISM. (d) Chemical structure of poly(styrene sulfonate) sodium salt

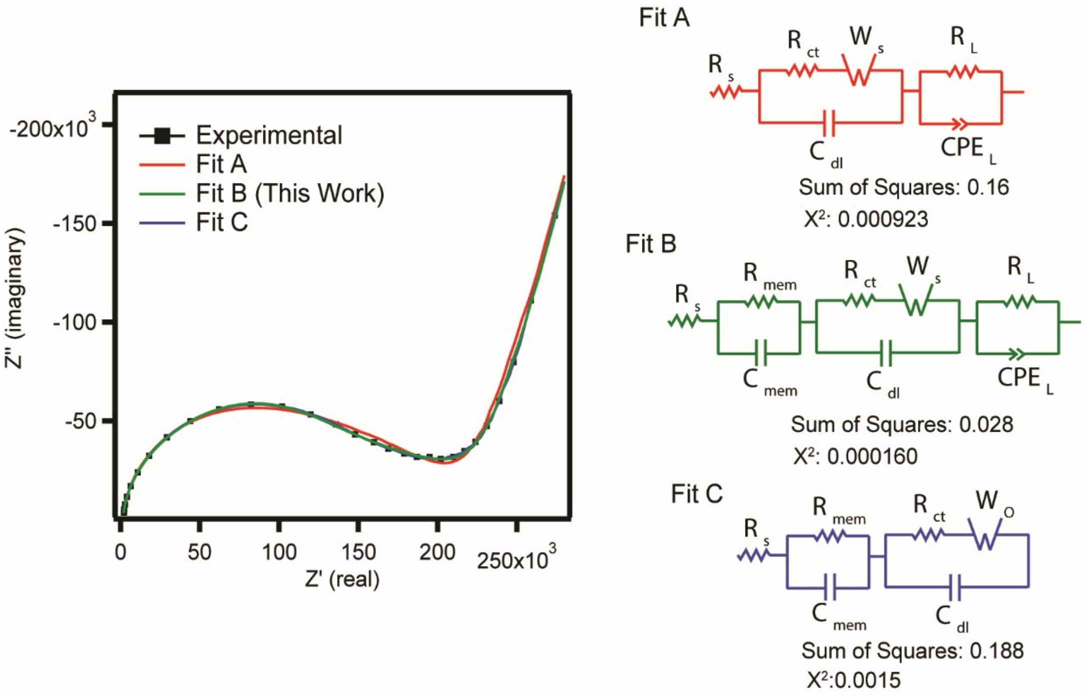

Figure S11. Experimental EIS response (black squares) of a HOIP pellet between ISM coated conductive ITO substrates showing fit comparison between different models. Fit A (Red), adapted from literature for supercapacitors, provides a good fit, however, deviates from the model in the high and mid-frequency range. Fit B is the model adapted from A, with an *R-C* component added in the high-frequency to account for bulk resistance capacitance of the membranes. Fit B provides the best fit to the model with lowest sum of square and χ^2 values. Fit C shows the same model in B where the low frequency component is replaced by an open Warburg component, to model ion diffusion to a blocking boundary. This would be the case for ion diffusion to ITO. However, Fit C does not show a better fit to the data, thus, we assume the low frequency feature due to ion diffusion to an adsorbing boundary as shown in Fit B.